


A Relativistic Complex Optical Potential Calculation for Electron–Beryllium Scattering: Recommended Cross Sections

Cite as: J. Phys. Chem. Ref. Data **47**, 033103 (2018); <https://doi.org/10.1063/1.5047139>
Submitted: 04 July 2018 . Accepted: 21 August 2018 . Published Online: 12 September 2018

R. P. McEachran, F. Blanco, G. García, and M. J. Brunger

COLLECTIONS

 This paper was selected as Featured



View Online



Export Citation



CrossMark

ARTICLES YOU MAY BE INTERESTED IN

[Integral Cross Sections for Electron–Magnesium Scattering Over a Broad Energy Range \(0–5000 eV\)](#)

Journal of Physical and Chemical Reference Data **47**, 043104 (2018); <https://doi.org/10.1063/1.5081132>

[Reference Values and Reference Correlations for the Thermal Conductivity and Viscosity of Fluids](#)

Journal of Physical and Chemical Reference Data **47**, 021501 (2018); <https://doi.org/10.1063/1.5036625>

[Reference Correlation of the Viscosity of n-Hexadecane from the Triple Point to 673 K and up to 425 MPa](#)

Journal of Physical and Chemical Reference Data **47**, 033102 (2018); <https://doi.org/10.1063/1.5039595>

Where in the **world** is AIP Publishing?
Find out where we are exhibiting next



A Relativistic Complex Optical Potential Calculation for Electron–Beryllium Scattering: Recommended Cross Sections

R. P. McEachran

Plasma Research Laboratory, Research School of Physics and Engineering, Australian National University, Canberra, Australian Capital Territory 0200, Australia

F. Blanco

Departamento de Física Atómica, Molecular y Nuclear, Universidad Complutense de Madrid, Avenida Complutense, E-28040 Madrid, Spain

G. García

Instituto de Física Fundamental, CSIC, Serrano 113-bis, E-28006 Madrid, Spain

M. J. Brunger^{a)}

College of Science and Engineering, Flinders University, GPO Box 2100, Adelaide, South Australia 5042, Australia

(Received 4 July 2018; accepted 21 August 2018; published online 12 September 2018)

We report results from the application of the relativistic complex optical potential (ROP) method to electron–beryllium scattering. The energy range of this study was 0–5000 eV, with the results for the integral elastic cross sections, momentum transfer cross sections, summed discrete electronic-state excitation integral cross sections, and total ionisation cross sections (TICSs) being reported. However we will largely focus our discussion here on the TICS, due to its importance in simulating the plasma action on beryllium (Be) in the international thermonuclear reactor. The current level of agreement between the various theoretical approaches to calculating the TICS is well summarised in the work of Maihom *et al.* [Eur. Phys. J. D **67**, 2 (2013)] and Blanco *et al.* [Plasma Sources Sci. Technol. **26**, 085004 (2017)], with the level of accord between them being quite marginal. As a consequence, we revisit this problem with improved scattering potentials over those employed in the work of Blanco *et al.* In addition, we present results from an application of the binary-encounter-Bethe theory for the electron–Be TICS. We find a quite significant improvement in the level of agreement between the TICS from our new ROP calculation and the earlier B-spline R-matrix and convergent close coupling results [O. Zatsarinny *et al.*, J. Phys. B: At., Mol. Opt. Phys. **49**, 235701 (2016)], compared to that reported in the work of Blanco *et al.* As a result of this improved level of accord, we propose here a recommended TICS for e + Be scattering, as well as for the elastic integral and summed electronic-state excitation cross sections, which also incorporates uncertainty estimates for their validity. *Published by AIP Publishing on behalf of the National Institute of Standards and Technology.* <https://doi.org/10.1063/1.5047139>

Key words: beryllium; electron scattering cross sections; recommended cross sections.

CONTENTS

1. Introduction	2	2. Theoretical Details	3
		2.1. ROP calculation	3
		2.2. BEB calculation	3
		3. Uncertainty Estimates	4
		4. Results and Discussion	4
		5. Conclusions	11
		Acknowledgments	12
		6. References	12

^{a)}Author to whom correspondence should be addressed: michael.brunger@flinders.edu.au

Published by AIP Publishing on behalf of the National Institute of Standards and Technology.

List of Tables

1.	A selection of the present theoretical ROP results ($\times 10^{-16} \text{ cm}^2$) for electron scattering from Be. . .	5
2.	Our recommended elastic ICSs, summed electronic-state excitation ICSs, and the TICSs for electron–Be scattering (all in units of 10^{-16} cm^2) on a fine energy grid.	6

List of Figures

1.	Present status for theoretical electron–Be TICS calculation results	2
2.	TICSs for electron–Be scattering, including our new ROP and BEB results	4
3.	Summary plot of our recommended cross section data ($\times 10^{-16} \text{ cm}^2$) for e^- –Be scattering	11

1. Introduction

It is now well known that beryllium (Be) will be one of the materials exposed to the plasma in the international thermonuclear experimental reactor (ITER).¹ This exposure will lead to the formation of gas-phase Be, with its presence in the fusion edge and divertor plasmas influencing their behaviour due, amongst others, to electron collision processes.² Those processes are quantified by their relevant electron scattering cross sections, in particular, the total ionisation cross section (TICS), which therefore become crucial inputs when attempting to simulate the effect the plasma might have on the materials that are exposed to it.

As a consequence of the above, there has been significant theoretical activity in attempting to calculate cross sections for electron scattering from Be. Focussing on the TICS here, we note plane wave Born approximation (PWBA) results that can be obtained from the method in the work of Deutsch *et al.*,^{3,4} a distorted-wave with electron scattering (DWIS(N-1)) computation from the work of Bartlett and Stelbovics,⁵ a Deutsch–Märk (DM) calculation from the work of Maihom *et al.*,² the close coupling (CC) and R-matrix with pseudo-states (RMPS) results from the work of Zakrzewski and Ortiz,⁶ a later convergent close coupling (CCC) and a new B-spline R-matrix (BSR) calculation from the work of Zatsarinny *et al.*,⁷ and our own optical potential (OP) computation (Blanco *et al.*).⁸ Note that as Be is not a particularly easy material to work with, there are no experimental cross sections currently available in the literature for it. All the earlier theoretical TICS^{3–8} are now plotted in Fig. 1, so as to give the reader a clear picture of the extent of the agreement between them. It is apparent from Fig. 1 that while some of the theoretical results are in quite good agreement with some of the others, in general there is a rather wide divergence in the reported absolute values for the TICS. For example, at the energy where a maximum in the cross section is found, the variance in the magnitude of that TICS can be as much as a factor of two. Therefore we have decided to revisit this scattering system, using our relativistic complex optical potential (ROP) method⁹ and with improved scattering potentials (see later) over those employed in the work of Blanco *et al.*,⁸ in order to try and further clarify this situation. Furthermore, as is evident from Fig. 1, many of the available theories only go up to 100 eV incident electron energy. To be useful in modeling applications, particularly with respect to high-temperature plasmas, a much larger energy range is required. Therefore, another rationale for the present ROP calculation is to hopefully enable us to extend the cross

section data to those higher energies. In addition to our ROP computation, we also report new binary encounter Bethe (BEB) calculation results, as there is a large body of data that suggest that this quite simple approach can provide remarkably accurate ionisation cross sections.¹⁰ Finally we will present a recommended TICS for electron–Be scattering, with uncertainty limits, over an extended energy range for use in simulation studies. Recommended data for elastic scattering and the summed electronic-state excitation cross section, with associated confidence limits, will also be provided.

The structure for the remainder of this short paper is as follows. In Sec. 2, we describe our ROP and BEB calculations, while in Sec. 3, we discuss the uncertainty estimates we quote on our recommended data. The present computational results and a discussion of these results are given in Sec. 4. Also included in Sec. 4 will be our recommended elastic integral cross section (ICS), summed electronic-state excitation ICS, and TICS values for this scattering system, with uncertainty estimates on those cross sections additionally being provided. Finally, in Sec. 5, some conclusions from the present investigation will be given.

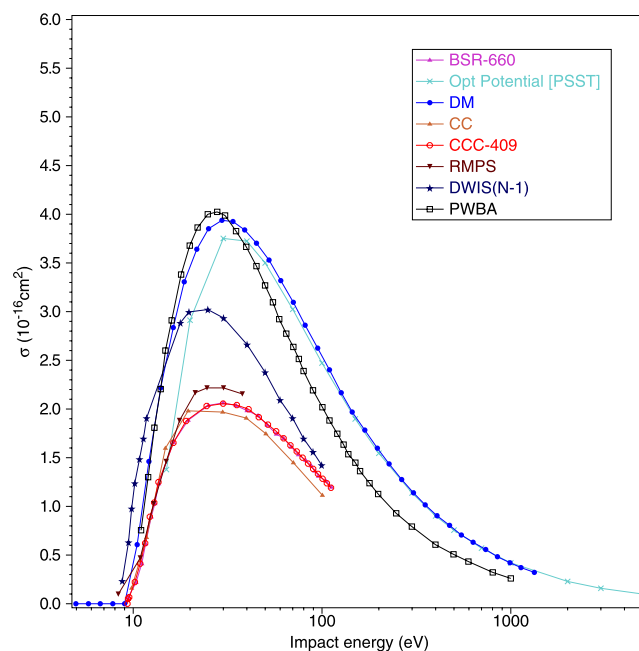


FIG. 1. Present status for theoretical electron–Be TICS calculation results. See the legend for further details.

2. Theoretical Details

2.1. ROP calculation

In this work, the elastic and absorption cross sections were calculated using a ROP method. This method was originally developed by Chen *et al.*⁹ and used to calculate total and differential cross sections as well as spin polarisation parameters for relatively low energy electrons and positrons incident upon krypton. That paper will be referred to as I hereafter. It has subsequently been successfully used in several different fields of atomic scattering, in particular, in the analysis of energy-loss spectra at several keV by Vos *et al.*,¹¹ in the investigation of the behaviour of the Sherman function in electron scattering from xenon,¹² for low energy positron interactions with krypton,¹³ and for positronium formation in the noble gases.¹⁴

The ROP method is based upon the solution of the Dirac scattering equations. Here the radial integral equations for the large and small components of the scattering wavefunctions, $F_0(x)$ and $G_0(x)$, can be expressed in matrix form as

$$\begin{pmatrix} F_0(x) \\ G_0(x) \end{pmatrix} = \begin{pmatrix} v_1(k_0x) \\ v_2(k_0x) \end{pmatrix} + \frac{1}{k_0} \int_0^x dr G_{T_0}^P(x, r) \times \left[U(r) \begin{pmatrix} F_0(r) \\ G_0(r) \end{pmatrix} - \begin{pmatrix} \overline{W}_P(\kappa_2; r) \\ \overline{W}_Q(\kappa_2; r) \end{pmatrix} - i U_{\text{abs}}(r) \begin{pmatrix} F_0(r) \\ G_0(r) \end{pmatrix} \right]. \quad (1)$$

In Eq. (1), the local potential $U(r)$ is the sum of the static and polarization potentials, while $\overline{W}_P(\kappa_2; r)$ and $\overline{W}_Q(\kappa_2; r)$ are the large and small components of the non-local exchange terms. Finally, $U_{\text{abs}}(r)$ is the non-local absorption potential and is determined as an expansion over the inelastic channels of the target atom. These inelastic channels include both excitation of the higher lying bound states and single ionisation of the target as given by Eq. (21b) of I. The above Green's function $G_{T_0}^P(x, r)$ can be expressed in terms of Riccati-Bessel and Riccati-Neumann functions [see Eq. (23) of I for details]. The angular momentum quantum number $\kappa_2 = \pm 1, \pm 2, \dots$ of the incident electron can be defined in terms of its orbital angular quantum number l_2 and the total angular momentum quantum number j_2 according to $j_2 = |\kappa_2| - \frac{1}{2}$ with $l_2 = \kappa_2$ if $\kappa_2 > 0$ and $l_2 = -\kappa_2 - 1$ if $\kappa_2 < 0$.

In particular, the polarization potential was determined by the polarized-orbital method^{15,16} and included the first 7 multipole potentials plus the corresponding dynamic polarization potential.¹⁷ Thus, asymptotically the polarization potential contained all terms up to and including those corresponding to r^{-14} .

The ground state wavefunction of beryllium was determined in a single configuration calculation using the multi-configuration Dirac-Fock (MCDF) programme of Grant *et al.*¹⁸ This wavefunction was used in the calculation of the static potential as well as the bound and continuum state

coupling potentials in the absorption potential. For the excited bound states of beryllium, which were used in the absorption potential, we included those 10 states where one of the electrons in the outer 2s valence shell was excited to a higher lying $np^{1,3}P$ state with $n = 2-6$ inclusive. For the case of ionisation, we included those continuum states which correspond to an orbital angular momentum of 0-4; this gives rise to up to 49 ionisation channels depending on the total angular momentum of the incident electron.

Equation (1) was solved iteratively to obtain the complex phase shifts $\eta_{l_2}^{\pm} = \delta_{l_2}^{\pm} + i\gamma_{l_2}^{\pm}$ with $\gamma_{l_2}^{\pm} \geq 0$. Here the (+) sign corresponds to "spin-up" ($j_2 = l_2 + \frac{1}{2}$) and the (-) sign corresponds to "spin-down" ($j_2 = l_2 - \frac{1}{2}$). In terms of these phase shifts, the elastic cross section is given by

$$\sigma^{\text{el}}(k^2) = \frac{2\pi}{k^2} \sum_{l_2=0}^{\infty} \{ (l_2 + 1) \exp(-2\gamma_{l_2}^+) [\cosh 2\gamma_{l_2}^+ - \cos 2\delta_{l_2}^+] + l_2 \exp(-2\gamma_{l_2}^-) [\cosh 2\gamma_{l_2}^- - \cos 2\delta_{l_2}^-] \}, \quad (2)$$

while the absorption cross section is given by

$$\sigma^{\text{abs}}(k^2) = \frac{\pi}{k^2} \sum_{l_2=0}^{\infty} \{ (l_2 + 1) [1 - \exp(-4\gamma_{l_2}^+)] + l_2 [1 - \exp(-4\gamma_{l_2}^-)] \}. \quad (3)$$

Here k is the relativistic wavenumber of the incident electron.

2.2. BEB calculation

The BEB approach for atomic systems is well described in the recent review of Tanaka *et al.*,¹⁰ and so we do not go into detail here. Rather we note that the ionisation cross section for a particular orbital ($2s^2$ here for Be) is given by

$$\sigma_{\text{BEB}}(t) = \frac{S}{t+u+1} \left[\frac{\ln(t)}{2} \left(1 - \frac{1}{t^2} \right) + 1 - \frac{1}{t} - \frac{\ln(t)}{t+1} \right], \quad (4)$$

where $t = TB$, $u = UB$, $S = 4\pi a_0^2 NR^2/B^2$, a_0 is the Bohr radius (0.529 Å), R is the Rydberg energy (13.6057 eV), and T is the incident electron energy. N , B , and U are the electron occupation number, the binding energy (ionisation potential = 9.3227 eV¹⁹), and the average kinetic energy of the orbital, respectively. In this case, we have used the experimental value of the ionisation potential (from the ground $2s^2$ state) for B , while N and U are determined from a DFT computation at the B3LYP level with GAUSSIAN.²⁰ The present BEB TICS is plotted in Fig. 2. Note that there was an earlier BEB electron-Be TICS from the work of Maihom *et al.*,² with a Hartree-Fock model chemistry. The BEB result in the work of Maihom *et al.* differs from the present, largely in terms of the magnitude of the TICS at its maximum value (they are ~20% higher in value), by more than one would anticipate simply on the basis of the different model chemistries used in the two calculations. We have checked our BEB result very carefully and believe it is correct. As a consequence, the earlier result² has not been included in either Fig. 1 or Fig. 2.

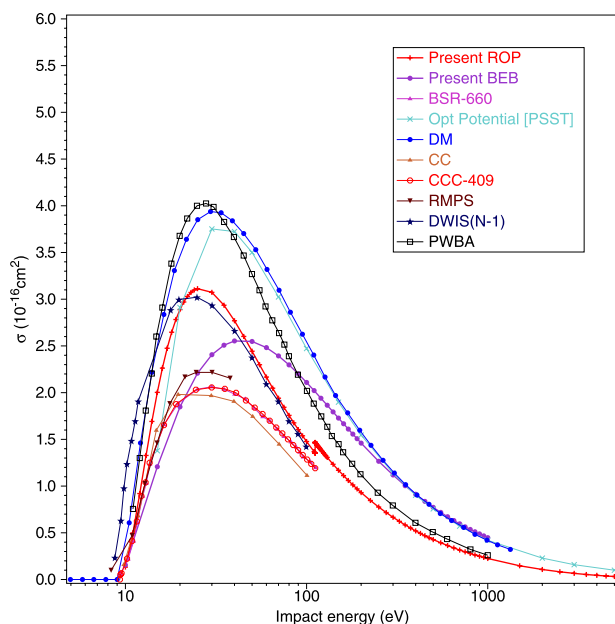


FIG. 2. TICSs for electron–Be scattering, including our new ROP and BEB results. See the legend for further details.

3. Uncertainty Estimates

It is very important for the modeling community to have uncertainty limits on the recommended cross section data, when they come to apply those cross sections to the application of interest.²¹ In this case, we are proposing recommended data from theory alone, and given that all the theories have been properly applied and are converged their intrinsic uncertainties are probably 1% or less. Under these circumstances, we have adopted as our uncertainties the confidence limits that are typically associated with benchmark experiments, if such experiments were in fact possible for electron–Be scattering. Those experimental uncertainties are detailed in the work of Buckman *et al.*²² and typically are $\pm 10\%$ for elastic scattering, $\pm 30\%$ for electronic-state excitation, and $\pm 5\%$ for the TICS. In the present application, however, we have formed the confidence limits on the TICS from the standard deviation on the average values, at each energy, of the six theoretical results [CC, CCC, BSR, RMPS, DWIS(N-1), and ROP] we employed to determine the recommended ionisation data below 100 eV (see later). This approach led to a conservative $\pm 20\%$ uncertainty on our recommended TICS. Note that while that estimate is conservative, it is not unreasonable. Recent TICS measurements with the primary alcohols,^{23–25} which are liquids at room temperature, reported uncertainties up to $\sim 12\%$. As any measurements with beryllium would be a degree of difficulty more challenging, our $\pm 20\%$ uncertainty estimate on our recommended TICS is highly plausible.

4. Results and Discussion

In Table 1, we present a summary of all the present ROP calculation results for electron–Be scattering. These consist

of data for the elastic ICS, for energies in the range 0–5000 eV, the momentum transfer cross section (MTCS), again for energies between 0 and 5000 eV, the summed electronic-state excitation cross sections, for energies from threshold (2.8 eV) to 5000 eV, and the TICS, for energies from its threshold (~ 10 eV) to 5000 eV. Note that we do not discuss our MTCS results further, but they are included in Table 1 because in some modeling applications they are important parameters. One important example of this is in simulating electron transport under an applied external electric field through the background gas of interest (i.e., swarm physics).^{26–29} While we do not explicitly include plots of the available theoretical ICS results for either elastic scattering^{7,8} or the summed electronic-states,^{7,8,30} it would be remiss of us not to provide a brief summary of their current status.

For the elastic ICS, the BSR and CCC results were found to be in good agreement over their common energy range ($< 10\%$ difference) and, for energies above about 2 eV (to $\sim 10\%$ or better) and up to 100 eV, were also found to be in good agreement with the optical model result from the work of Blanco *et al.*⁸ This good level of accord between the sophisticated BSR method and the OP model approach, in the elastic channel, is by no means unique, having been also seen earlier for electron–atomic iodine scattering.³¹ The present ROP elastic ICS reinforces this scenario, being in very good agreement with the BSR result over their entire common energy range (0–100 eV) to typically better than 20% [with the worst agreement being at the lowest common energies (~ 0.01 eV–0.2 eV)]. As a consequence of this level of accord, we can construct a recommended elastic $e^- + \text{Be}$ scattering cross section that is composed of the BSR result for energies between 0 and 100 eV and our current ROP result for energies between 100 and 5000 eV. A selection of these recommended elastic ICS results is given in Table 2 with the estimated uncertainty on them being $\pm 10\%$.

The situation with respect to the sum of electronic-excited states is, however, much less clear. While the BSR and CCC results are typically again in good accord, to better than 10%, from threshold to 100 eV, the OP result of Blanco *et al.*⁸ is very different from them both. While we would anticipate a divergence between them near-threshold where the OP model, with a local-exchange potential to describe exchange scattering and a standard description for the polarisation potential, is known to be less accurate,⁸ the factor of 4 difference at 100 eV was highly surprising and indeed formed an important rationale for the present ROP application. When we compare our current summed electronic-state excitation ROP ICS to the earlier results,^{7,8} we find fair agreement, across most of the common energy range from threshold–100 eV, with the CCC and BSR calculations. The only exception to this general claim is near-threshold, where our $2s^2 \rightarrow 2s2p\ 2^3P$ excitation is apparently much smaller than the corresponding BSR cross section.

The excitation of the 2^3P state in Be, under a LS-coupling scheme, would be via the exchange interaction, and this would normally be expected to be much smaller in magnitude than the dipole-allowed 2^1P excitation. However, here there are some strong near-threshold resonance states,³² found in both the CCC and BSR computations, which greatly enhance

TABLE 1. A selection of the present theoretical ROP results ($\times 10^{-16} \text{ cm}^2$) for electron scattering from Be. Here the acronym MTCS denotes the momentum transfer cross section

Energy (eV)	Elastic ($\times 10^{-16} \text{ cm}^2$)	Inelastic ($\times 10^{-16} \text{ cm}^2$)	TICS ($\times 10^{-16} \text{ cm}^2$)	MTCS ($\times 10^{-16} \text{ cm}^2$)
0	0.005	0	0	0.005
0.04	16.619	0	0	25.252
0.08	44.17	0	0	63.892
0.12	94.666	0	0	126.592
0.16	181.729	0	0	223.249
0.19	272.871	0	0	315.051
0.22	371.223	0	0	404.166
0.26	464.859	0	0	470.959
0.32	467.746	0	0	431.341
0.36	420.658	0	0	367.506
0.4	369.764	0	0	307.931
0.44	325.47	0	0	259.773
0.48	289.403	0	0	222.442
0.6	218.36	0	0	153.378
0.8	161.183	0	0	102.676
1	132.521	0	0	79.569
1.4	102.779	0	0	58.029
2	80.408	0	0	43.894
2.6	67.174	0	0	36.323
2.9	58.459 983	0.023 778	0	33.975 614
4	50.382 931	0.034 919	0	28.198 544
4.8	45.880 451	0.033 316	0	24.67 233
5.6	41.518 683	1.432 638	0	20.543 089
6	39.326 243	3.557 447	0	17.744 882
6.8	35.962 291	7.095 222	0	13.638 445
7.6	33.072 483	9.864 948	0	10.87 313
8.4	30.520 351	12.009 985	0	8.959 686
9.2	28.215 034	13.860 551	0	7.525 776
13	20.52 985	17.40 913	1.32 778	4.18 305
17	16.08 154	17.81 907	2.47 498	2.88 006
21	13.44 764	17.79 879	2.97 001	2.25 224
25	11.65 655	17.27 077	3.11 284	1.90 206
45	7.53 309	14.15 983	2.60 157	1.10 884
65	5.8 253	11.84 275	2.04 774	0.78 744
85	4.8 296	9.95 909	1.67 695	0.60 173
111	3.99 371	8.23 668	1.35 893	...
111.4	3.98 333	8.21 431	1.35 501	...
111.5175	3.92 773	8.18 855	1.46 583	...
112	3.9 154	8.16 178	1.46 184	...
118	3.76 908	7.84 381	1.40 584	...
140	3.31 938	6.86 087	1.23 353	0.32 279
180	2.73 724	5.68 814	1.01 253	0.23 373
250	2.10 127	4.36 431	0.77 566	0.14 837
300	1.8 039	3.66 582	0.66 603	0.11 377
400	1.40 685	2.70 648	0.52 033	0.07 363
500	1.15 345	2.09 458	0.4 271	0.052
700	0.8 483	1.46 152	0.31 567	0.03 035
1000	0.60 772	0.92 789	0.22 499	0.01 711
3000	0.21 005	0.17 381	0.06 571	0.00 255
5000	0.12 696	0.07 769	0.03 231	0.00 103

the magnitude of the 2^3P state excitation cross section. As the present ROP calculation includes only a relatively small number of excited states, it cannot replicate this type of resonance. Therefore, to construct our recommended data set, we prefer the BSR and CCC results in this near-threshold energy regime. However, above the near-threshold region, the level of accord between our ROP and the BSR calculation is typically better than 30% up to 100 eV. As a consequence, we believe we are now in a position to recommend a summed electronic-state excitation ICS for e^- -Be scattering. This recommended ICS is formed from the BSR results from

threshold to 70 eV, and for $E_0 = 70$ –1000 eV from the present ROP computation (scaled downwards by a factor of 0.64 at 70 eV to ensure continuity). Note that we have truncated the BSR cross sections at 70 eV due to some convergence issues with their higher energy data for the excited electronic-states. In the energy range 1000–5000 eV we prefer the cross sections from the Livermore computation,³⁰ due to their clearly exhibiting the anticipated Born-like high-energy asymptotic behaviour. Values for a selection of our recommended ICS here can also be found in Table 2, with the uncertainty limits of those data now being $\pm 30\%$.

TABLE 2. Our recommended elastic ICSs, summed electronic-state excitation ICSs, and the TICSs for electron-Be scattering (all in units of 10^{-16} cm^2) on a fine energy grid. The uncertainties on the elastic ICS are $\sim \pm 10\%$, the uncertainties on the summed electronic state excitation ICS are $\sim \pm 30\%$, and the uncertainties on the TICS are $\sim \pm 20\%$

Energy (eV)	Elastic ($\times 10^{-16} \text{ cm}^2$)	Inelastic ($\times 10^{-16} \text{ cm}^2$)	TICS ($\times 10^{-16} \text{ cm}^2$)
$2.643\,080 \times 10^{-4}$	3.498 32		
$5.292\,000 \times 10^{-4}$	2.010 29		
$8.026\,390 \times 10^{-4}$	1.633 18		
$1.059\,571 \times 10^{-3}$	1.455 15		
$1.335\,457 \times 10^{-3}$	1.389 50		
$2.673\,868 \times 10^{-3}$	1.357 79		
$4.055\,459 \times 10^{-3}$	1.489 13		
$5.353\,527 \times 10^{-3}$	1.633 18		
$6.747\,610 \times 10^{-3}$	1.832 98		
$8.119\,887 \times 10^{-3}$	2.057 23		
$9.771\,247 \times 10^{-3}$	2.256 23		
$1.071\,890 \times 10^{-2}$	2.474 48		
$1.231\,544 \times 10^{-2}$	2.713 84		
$1.414\,979 \times 10^{-2}$	3.045 85		
$2.704\,955 \times 10^{-2}$	6.375 45		
$4.102\,702 \times 10^{-2}$	11.094 6		
$5.415\,892 \times 10^{-2}$	16.051 3		
$6.826\,058 \times 10^{-2}$	22.692 9		
$8.214\,290 \times 10^{-2}$	30.635 1		
$9.437\,783 \times 10^{-2}$	38.589 6		
0.108 437	48.609 4		
0.118 953	59.832 9		
0.136 672	71.968 1		
0.164 467	104.121		
0.188 965	147.204		
0.197 916	173.021		
0.217 112	198.724		
0.227 397	228.244		
0.238 168	250.323		
0.249 451	280.944		
0.273 644	315.319		
0.300 184	345.820		
0.329 297	370.612		
0.344 896	388.124		
0.396 269	362.160		
0.434 701	322.678		
0.499 450	294.219		
0.523 110	268.269		
0.690 551	208.113		
0.793 409	169.071		
0.870 359	147.204		
1.096 99	128.165		
1.203 38	116.861		
1.448 12	104.121		
2.523 54	64.123 9		
2.768 29	54.555 7		
2.857 00		5.966 74	
2.993 05		11.904 0	
3.129 09		15.811 6	
3.265 14		16.649 9	
3.331 29	43.310 2		
3.401 19		15.983 6	
3.537 24		15.121 2	
3.673 28		14.303 5	
3.809 33		13.546 2	
3.945 38		12.919 4	
4.081 43		12.417 8	
4.198 71	36.007 3		
4.217 48		11.951 2	
4.353 52		11.447 4	
4.489 57		10.913 6	
4.625 62		10.404 8	
4.761 67		9.965 16	

TABLE 2. Our recommended elastic ICSs, summed electronic-state excitation ICSs, and the TICSs for electron-Be scattering (all in units of 10^{-16} cm^2) on a fine energy grid. The uncertainties on the elastic ICS are $\sim \pm 10\%$, the uncertainties on the summed electronic state excitation ICS are $\sim \pm 30\%$, and the uncertainties on the TICS are $\sim \pm 20\%$ —Continued

Energy (eV)	Elastic ($\times 10^{-16} \text{ cm}^2$)	Inelastic ($\times 10^{-16} \text{ cm}^2$)	TICS ($\times 10^{-16} \text{ cm}^2$)
4.897 71		9.603 64	
5.033 76		9.301 50	
5.169 81		9.042 27	
5.305 86		9.213 33	
5.441 90		8.806 44	
5.577 95		8.569 14	
5.714 00		8.407 21	
5.805 22	28.585 1		
5.850 05		8.302 30	
5.986 09		8.276 79	
6.122 14		8.456 81	
6.258 19		8.444 18	
6.394 24		8.338 91	
6.530 28		8.456 19	
6.666 33		8.506 89	
6.802 38		8.517 90	
6.938 43		8.678 92	
7.074 47		8.873 18	
7.210 52		9.125 21	
7.346 57		8.983 78	
7.482 62		9.132 76	
7.618 66		9.323 67	
7.754 71		9.404 20	
7.890 76		9.639 17	
8.026 44	23.222 6		
8.026 81		9.667 19	
8.162 86		9.930 27	
8.298 90		10.136 1	
8.434 95		10.247 2	
8.571 00		10.603 6	
8.707 05		10.604 0	
8.843 09		10.719 0	
8.979 14		10.848 1	
9.115 19		11.071 2	
9.251 24		11.099 4	
9.387 28		11.161 2	
9.400 00			0.143 623
9.523 33		11.308 3	
10.000 0			0.325 492
10.116 5	20.219 0		
10.203 6		11.710 8	
10.237 7			0.397 555
10.481 1			0.468 432
10.730 3			0.544 638
10.883 8		11.719 4	
10.985 4			0.622 755
11.246 6			0.711 917
11.514 0			0.810 643
11.564 0		11.621 0	
11.787 7			0.912 698
12.067 9			1.004 00
12.173 9	16.426 3		
12.244 3		11.549 1	
12.354 8			1.093 55
12.648 6			1.173 16
12.924 5		11.441 4	
12.949 3			1.251 58
13.257 1			1.341 88
13.572 3			1.436 84
13.604 8		11.363 4	
13.895 0			1.511 30
13.987 2	14.635 6		
14.225 3			1.580 46

TABLE 2. Our recommended elastic ICSs, summed electronic-state excitation ICSs, and the TICSs for electron-Be scattering (all in units of 10^{-16} cm^2) on a fine energy grid. The uncertainties on the elastic ICS are $\sim \pm 10\%$, the uncertainties on the summed electronic state excitation ICS are $\sim \pm 30\%$, and the uncertainties on the TICS are $\sim \pm 20\%$ —Continued

Energy (eV)	Elastic ($\times 10^{-16} \text{ cm}^2$)	Inelastic ($\times 10^{-16} \text{ cm}^2$)	TICS ($\times 10^{-16} \text{ cm}^2$)
14.563 5			1.650 32
14.909 7			1.718 08
15.264 2			1.776 00
15.627 1			1.834 50
15.998 6			1.894 39
16.325 7		10.997 7	
16.378 9			1.951 05
16.768 3			1.995 23
17.167 0			2.039 32
17.575 1			2.082 84
17.992 9			2.123 28
18.420 7			2.158 80
18.464 2	10.841 5		
18.858 6			2.195 12
19.046 7		10.768 0	
19.307 0			2.228 43
19.766 0			2.253 83
20.235 9			2.267 97
20.717 0			2.281 44
21.209 5			2.294 49
21.713 7			2.306 83
22.230 0			2.318 79
22.758 5			2.330 17
23.299 5			2.341 08
23.853 4			2.351 65
24.374 2	8.807 69		
24.420 5			2.361 50
24.488 6		10.222 4	
25.001 1			2.368 61
25.595 5			2.367 82
26.204 0			2.366 74
26.827 0			2.365 65
27.464 7			2.364 52
28.117 7			2.363 37
28.786 2			2.362 19
29.470 5			2.360 99
29.930 5		9.784 73	
30.171 1			2.357 63
30.721 3	7.155 45		
30.888 4			2.348 74
31.622 8			2.339 64
32.374 6			2.330 33
33.144 2			2.320 79
33.932 2			2.311 02
34.738 9			2.301 03
35.372 4		9.263 35	
35.564 8			2.289 20
36.410 3			2.275 77
37.275 9			2.262 02
38.162 1			2.247 95
39.069 4			2.233 53
39.998 2			2.218 34
40.554 6	6.229 97		
40.814 3		8.951 07	
40.949 1			2.201 85
41.922 7			2.183 99
42.919 3			2.165 70
43.939 7			2.146 97
44.984 3			2.127 80
46.053 8			2.107 85
46.256 2		8.582 05	
46.595 1	5.300 43		
47.148 7			2.084 92

TABLE 2. Our recommended elastic ICSs, summed electronic-state excitation ICSs, and the TICSs for electron-Be scattering (all in units of 10^{-16} cm^2) on a fine energy grid. The uncertainties on the elastic ICS are $\sim \pm 10\%$, the uncertainties on the summed electronic state excitation ICS are $\sim \pm 30\%$, and the uncertainties on the TICS are $\sim \pm 20\%$ —Continued

Energy (eV)	Elastic ($\times 10^{-16} \text{ cm}^2$)	Inelastic ($\times 10^{-16} \text{ cm}^2$)	TICS ($\times 10^{-16} \text{ cm}^2$)
48.2696			2.061 48
49.4171			2.037 48
50.5920			2.013 22
51.6981		8.122 04	
51.7947			1.989 22
53.0261			1.965 54
54.2868			1.941 31
55.5774			1.916 74
56.8987			1.891 91
57.1400		7.858 74	
58.2514			1.868 47
58.7273	4.509 57		
59.6362			1.845 47
61.0540			1.824 24
62.5055			1.803 13
62.5819		7.645 66	
63.9915			1.778 81
65.5128			1.753 70
67.0704			1.728 39
68.0238		7.375 33	
68.6649			1.702 73
70.2973			1.677 66
71.9686			1.652 89
73.6796			1.627 66
75.0000		6.941 10	
75.4312			1.602 59
77.2245			1.579 30
79.0604			1.555 48
80.0000		6.697 25	
80.9400			1.532 76
81.1989	3.749 17		
82.8643			1.510 23
84.8343			1.486 69
85.0000		6.415 16	
86.8511			1.463 34
88.9159			1.437 98
90.0000		6.153 26	
91.0298			1.411 39
93.1940			1.385 04
95.0000		5.910 41	
95.4095			1.358 40
97.6778			1.335 70
100.000		5.684 89	1.313 54
110.000	2.917 09	5.342 05	1.217 35
111.000	2.898 05	5.305 67	1.208 55
111.200	2.894 29	5.298 45	1.206 79
111.400	2.890 52	5.291 26	1.205 06
111.490	2.888 84	5.288 03	1.204 27
111.518	2.850 17	5.274 67	1.303 62
111.520	2.850 12	5.274 53	1.304 22
111.530	2.849 94	5.274 18	1.304 14
111.540	2.849 75	5.273 82	1.304 05
111.550	2.849 56	5.273 46	1.303 96
111.600	2.848 64	5.271 68	1.303 53
111.800	2.844 93	5.264 54	1.301 79
112.000	2.841 23	5.257 42	1.300 07
113.000	2.822 88	5.222 14	1.291 49
114.000	2.804 81	5.187 32	1.283 00
115.000	2.787 06	5.152 93	1.274 67
116.000	2.769 47	5.119 06	1.266 43
117.000	2.752 15	5.085 59	1.258 30
118.000	2.735 05	5.052 60	1.250 26
119.000	2.718 19	5.020 04	1.242 34

TABLE 2. Our recommended elastic ICSs, summed electronic-state excitation ICSs, and the TICSs for electron–Be scattering (all in units of 10^{-16} cm^2) on a fine energy grid. The uncertainties on the elastic ICS are $\sim \pm 10\%$, the uncertainties on the summed electronic state excitation ICS are $\sim \pm 30\%$, and the uncertainties on the TICS are $\sim \pm 20\%$ —Continued

Energy (eV)	Elastic ($\times 10^{-16} \text{ cm}^2$)	Inelastic ($\times 10^{-16} \text{ cm}^2$)	TICS ($\times 10^{-16} \text{ cm}^2$)
120.000	2.701 54	4.987 86	1.234 51
122.000	2.668 89	4.924 72	1.219 15
124.000	2.637 07	4.863 16	1.204 14
126.000	2.606 04	4.803 10	1.189 51
128.000	2.575 78	4.744 45	1.175 21
130.000	2.546 26	4.686 85	1.161 76
140.000	2.408 72	4.419 44	1.097 02
150.000	2.286 09	4.179 25	1.039 92
160.000	2.176 07	4.032 46	0.989 120
170.000	2.076 68	3.840 39	0.942 510
180.000	1.986 29	3.664 02	0.900 480
190.000	1.903 62	3.501 21	0.862 461
200.000	1.827 64	3.350 21	0.827 554
225.000	1.662 21	3.089 46	0.752 316
250.000	1.524 80	2.811 28	0.689 823
275.000	1.408 65	2.570 87	0.637 316
300.000	1.309 01	2.361 34	0.592 325
325.000	1.222 60	2.177 50	0.553 594
350.000	1.147 02	2.015 31	0.519 497
375.000	1.080 29	1.871 49	0.489 517
400.000	1.020 89	1.743 38	0.462 748
425.000	0.967 689	1.628 80	0.438 834
450.000	0.919 796	1.525 90	0.417 232
475.000	0.876 453	1.433 13	0.397 622
500.000	0.837 006	1.349 23	0.379 836
550.000	0.767 909	1.261 60	0.349 865
600.000	0.709 378	1.137 02	0.323 363
650.000	0.659 155	1.031 57	0.300 578
700.000	0.615 573	0.941 440	0.280 737
750.000	0.577 418	0.863 749	0.263 270
800.000	0.543 718	0.796 242	0.247 805
850.000	0.513 749	0.737 115	0.233 975
900.000	0.486 914	0.685 023	0.221 534
950.000	0.462 750	0.638 844	0.210 337
1000.00	0.440 995	0.597 702	0.200 092
1500.00	0.299 180	0.306 558	0.130 937
2000.00	0.226 469	0.203 726	$9.542\,578 \times 10^{-2}$
2500.00	0.182 212	0.147 086	$7.338\,803 \times 10^{-2}$
3000.00	0.152 424	0.111 960	$5.843\,829 \times 10^{-2}$
3500.00	0.131 010	$8.841\,623 \times 10^{-2}$	$4.772\,179 \times 10^{-2}$
4000.00	0.114 864	$7.173\,270 \times 10^{-2}$	$3.971\,776 \times 10^{-2}$
4500.00	0.102 252	$5.942\,296 \times 10^{-2}$	$3.357\,244 \times 10^{-2}$
5000.00	$9.212\,907 \times 10^{-2}$	$5.004\,412 \times 10^{-2}$	$2.873\,446 \times 10^{-2}$

Finally, in Fig. 2, we compare the present ROP and BEB results for the TICS to the other available theories.^{2–8} From our discussion above, we observed that both the BSR and CCC computations (as well as our ROP result) did a pretty good job in describing both the elastic scattering and summed electronic-state excitation processes. As a consequence, we shall frame the discussion that follows in relation to those theories. The present BEB result predicts a cross section magnitude that is some 20% higher than the CCC and BSR results (see Fig. 2), and the position in energy of that maximum is shifted somewhat higher compared to those other theories. Indeed the level of accord between our BEB results and the CCC and BSR⁷ calculations is really quite marginal and quite a bit worse than what is usually found using the BEB

method even though it is only a model (rather than *ab initio*) approach.¹⁰ The valence electronic structure of Be can be written as $[\text{core}]2s^2$, while that of magnesium (Mg) is $[\text{core}]3s^2$. Namely, they are both similar in that they possess a pair of s-electrons outside a core. It is well known from electron momentum spectroscopy³³ that the initial state configuration plays an important role in describing the Mg 3s momentum distribution.³⁴ Specifically, the 3s orbital is in fact not a pure “s-type” so that an s/p admixture is required to correctly reproduce the measured 3s momentum distribution.³⁴ If a similar effect were also occurring in Be, then our BEB result, which employs a pure $2s^2$ ground-state orbital, would be in error. This in turn might explain in part why it (and indeed the model DM result²) does not reproduce the TICS in

Fig. 2 to the level we would normally expect. Note that *a priori*¹⁰ we would not expect a PWBA result,^{3,4} except at very high energies, to describe well the ionisation process and this is precisely what we find in Fig. 2. The OP TICS from Blanco *et al.*⁸ predicts a peak maximum which is some 40% higher in magnitude than those of the BSR and CCC results⁷ and at an energy that is a little higher than that of the CCC and BSR. These discrepancies are in part addressed by the present ROP calculation. In particular, the energy at which the TICS maximum value occurs, from our ROP computation, is now in excellent agreement with those from the CCC, BSR, DWIS (N-1),⁵ and RMPS⁶ results. While the magnitude of the TICS maximum from our ROP result is still $\sim 30\%$ higher than that from the BSR or CCC calculation, this represents an improvement compared to that found by Blanco *et al.*⁸ with their OP method. We believe this improvement reflects the superior description for exchange and polarisation in our ROP method, compared to their corresponding forms in the work of Blanco *et al.*⁸ Another interesting aspect in Fig. 2 is the apparent “discontinuity” in the ROP TICS at around an energy of 110 eV. This “discontinuity” is in fact physical, corresponding to the opening of the 1s core ionisation channel.

If we consider Fig. 2 in more detail, then four of the *ab initio* TICS calculations (CC, CCC, RMPS, and BSR) are bunched together with a peak maximum $\sim 2 \times 10^{-16} \text{ cm}^2$, while the remaining two *ab initio* results (ROP, DWIS(N-1)) are bunched with a peak maximum $\sim 3 \times 10^{-16} \text{ cm}^2$. In terms of constructing a recommended TICS data base from these results and without any *a priori* prejudice as to the validity of one method over any other, in the energy range from threshold to 100 eV, we have simply taken the average of the CC, CCC, BSR, RMPS, DWIS(N-1) and ROP results. While it could be argued that the track records of the CCC and BSR approaches, in electron-atom scattering and for a range of scattering processes,³⁵ is such that some preference might be afforded to them, here we have declined to do so. Our rationale for this is that in those cases where the CCC and BSR methods have been shown to be highly successful, at least for a subset of the open scattering channels, they were able to be benchmarked against independent and accurate measurements. This is not the case here. As a consequence, we adopted the approach of Itikawa (e.g., Refs. 36 and 37) who, in the absence of any reliable experimental measurements, suggested a method that might be paraphrased as follows: reject what is inaccurate and average what remains. In doing so cite confidence limits that cover the recommended (averaged) data and all the theory results used to generate that average. In adopting the Itikawa approach here to determine a recommended TICS, we make the following observations. Of the six theories (below 100 eV) we employed to generate our average, four (CC, CCC, BSR, and RMPS) were bunched quite closely together with the remaining two [DWIS(N-1) and ROP] also being bunched together but at a somewhat higher magnitude (see Fig. 2). Thus in taking the average, the CC, CCC, BSR, and RMPS TICS results will be weighted more strongly than those from the DWIS(N-1) and ROP methods, in forming our recommended TICS data. In addition, with the uncertainty we cite on our recommended TICS (see Sec. III), all those theory

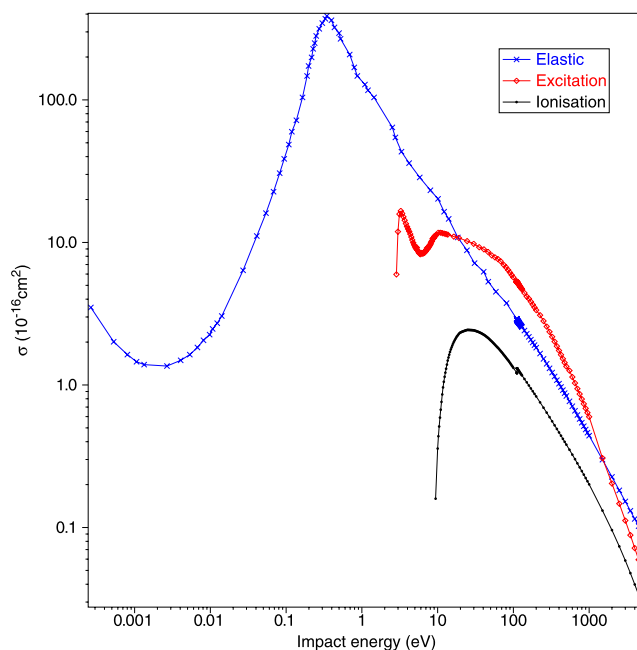


Fig. 3. Summary plot of our recommended cross section data ($\times 10^{-16} \text{ cm}^2$) for e^- -Be scattering. See also the legend.

results, including the CCC and BSR, are covered within those confidence limits about our recommended data. The uncertainty on that recommended data is then determined as the standard deviation calculated in taking that average. As the qualitative shapes of the TICS for all the CC, CCC, BSR, RMPS, DWIS(N-1),³⁻⁷ and ROP calculations are similar, we have used the form of the ROP result, suitably scaled ($\times 0.889$) to ensure continuity with the averaged data and to extrapolate the TICS from 100 eV to 5000 eV. A selection of the results of this process is also presented in Table 2, as are our confidence limits ($\pm 20\%$) for this recommended TICS.

In Fig. 3, we therefore provide a summary plot of our recommended cross sections for electron-Be scattering. A listing of all these data, on a fine energy grid, can also be found in Table 2. Note that a fine energy grid is crucial here, to enable modellers to perform an accurate numerical interpolation in order to extract the cross section data at the energies they require to undertake their simulation. This figure nicely illustrates the challenge faced by theory in describing this scattering system, where the magnitude of the ICSs can vary over several orders of magnitude in the energy range considered.

5. Conclusions

We have re-examined the available elastic ICSs, summed electronic-state excitation cross sections, and TICSs for e^- -Be scattering. In order to shed more light on some of the discrepancies between the existing theoretical data,²⁻⁸ we also undertook new ROP calculations over the 0–5000 eV energy range. As a result of these new computations, recommended cross section data for the above processes over a wide energy range and with confidence limits have also been determined as part of this study. We believe these recommended data will be very useful for modellers seeking to

better understand the possible action of the ITER plasma on its Be construction components. Finally, we highlight that by summing the recommended elastic ICS, summed electronic-state excitation ICS and TICS, at each energy, of Table 2 then a recommended total cross section for e^- -Be scattering can also be derived. In practice, however, this would be undertaken after a numerical interpolation of the listed data, in order to extract all those cross sections at each common energy to perform that summation.

Acknowledgments

This work was financially supported, in part, by the Spanish Ministerio de Economía y Competitividad (Project No. FIS2016-80440) and the Australian Research Council (Project Nos. DP160102787 and DP180101655). We thank Dr. L. Campbell and Dr. D. Jones for their help with some aspects of this study, while one of us (M.J.B.) thanks CSIC for its hospitality during a recent visit. Finally, we also thank Dr. O. Zatsarinny and Professor K. Bartschat for providing us tables of their BSR data.

6. References

- ¹G. Federici, *Phys. Scr.* **T124**, 1 (2006).
- ²T. Maihom, I. Sukuba, R. Janev, K. Becker, T. Märk, A. Kaiser, J. Limtrakul, J. Urban, P. Mach, and M. Probst, *Eur. Phys. J. D* **67**, 2 (2013).
- ³H. Deutsch, P. Scheier, S. Matt-Leubner, K. Becker, and T. D. Märk, *Int. J. Mass Spectrom.* **243**, 215 (2005).
- ⁴H. Deutsch, P. Scheier, S. Matt-Leubner, K. Becker, and T. D. Märk, *Int. J. Mass Spectrom.* **246**, 113 (2005).
- ⁵P. L. Bartlett and A. T. Stelbovics, *At. Data Nucl. Data Tables* **86**, 235 (2004).
- ⁶V. G. Zakrzewski and J. V. Ortiz, *J. Phys. Chem.* **100**, 13979 (1996).
- ⁷O. Zatsarinny, K. Bartschat, D. V. Fursa, and I. Bray, *J. Phys. B: At., Mol. Opt. Phys.* **49**, 235701 (2016).
- ⁸F. Blanco, F. Ferreira da Silva, P. Limão-Vieira, and G. García, *Plasma Sources Sci. Technol.* **26**, 085004 (2017).
- ⁹S. Chen, R. P. McEachran, and A. D. Stauffer, *J. Phys. B: At., Mol. Opt. Phys.* **41**, 025201 (2008).
- ¹⁰H. Tanaka, M. J. Brunger, L. Campbell, H. Kato, M. Hoshino, and A. R. P. Rau, *Rev. Mod. Phys.* **88**, 025004 (2016).
- ¹¹M. Vos, R. P. McEachran, C. Cooper, and A. P. Hitchcock, *Phys. Rev. A* **83**, 022707 (2011).
- ¹²R. P. McEachran, A. D. Stauffer, M. Piwinski, L. Preveca, J. F. Williams, D. Cvejanovic, and S. N. Samarm, *J. Phys. B: At., Mol. Opt. Phys.* **43**, 215208 (2010).
- ¹³C. Makochehanwa, J. R. Mackacek, A. C. L. Jones, P. Caradonna, D. S. Slaughter, R. P. McEachran, S. J. Buckman, B. Lohmann, D. F. Fursa, I. Bray, D. W. Meuller, A. D. Stauffer, and M. Hoshino, *Phys. Rev. A* **83**, 032721 (2011).
- ¹⁴R. P. McEachran and A. D. Stauffer, *J. Phys. B: At., Mol. Opt. Phys.* **46**, 075203 (2013).
- ¹⁵R. P. McEachran, D. L. Morgan, A. G. Ryman, and A. D. Stauffer, *J. Phys. B: At. Mol. Phys.* **10**, 663 (1977).
- ¹⁶R. P. McEachran, D. L. Morgan, A. G. Ryman, and A. D. Stauffer, *J. Phys. B: At. Mol. Phys.* **11**, 951 (1978).
- ¹⁷R. P. McEachran and A. D. Stauffer, *J. Phys. B: At., Mol. Opt. Phys.* **23**, 4605 (1990).
- ¹⁸I. P. Grant, B. J. McKenzie, P. H. Norrington, D. F. Mayer, and N. C. Pyper, *Comput. Phys. Commun.* **21**, 207 (1980).
- ¹⁹A. Kramida and W. C. Martin, *J. Phys. Chem. Ref. Data* **26**, 1185 (1997).
- ²⁰M. J. Frisch *et al.*, GAUSSIAN 09, Revision B.01, Gaussian, Inc., Wallingford, CT, USA, 2010.
- ²¹R. D. White, W. Tattersall, G. Boyle, R. E. Robson, S. Dujko, Z. Lj. Petrovic, A. Bankovic, M. J. Brunger, J. P. Sullivan, S. J. Buckman, and G. Garcia, *Appl. Radiat. Isotopes* **83**, 77 (2014).
- ²²S. J. Buckman, M. J. Brunger, and K. Ratnavelu, *Fusion Sci. Technol.* **63**, 385 (2013).
- ²³K. L. Nixon, W. A. D. Pires, R. F. C. Neves, H. V. Duque, D. B. Jones, M. J. Brunger, and M. C. A. Lopes, *Int. J. Mass Spectrom.* **404**, 48 (2016).
- ²⁴W. A. D. Pires, K. L. Nixon, S. Ghosh, R. F. C. Neves, H. V. Duque, R. A. A. Amorim, D. B. Jones, F. Blanco, G. Garcia, M. J. Brunger, and M. C. A. Lopes, *Int. J. Mass Spectrom.* **422**, 32 (2017).
- ²⁵S. Ghosh, K. L. Nixon, W. A. D. Pires, R. A. A. Amorim, R. F. C. Neves, H. V. Duque, D. G. M. da Silva, D. B. Jones, F. Blanco, G. Garcia, M. J. Brunger, and M. C. A. Lopes, *Int. J. Mass Spectrom.* **430**, 44 (2018).
- ²⁶R. D. White, D. Cocks, G. Boyle, M. Casey, N. Garland, D. Konovalov, B. Philippa, P. Stokes, J. de Urquijo, O. González-Magaña, R. P. McEachran, S. J. Buckman, M. J. Brunger, G. Garcia, S. Dujko, and Z. Lj. Petrovic, *Plasma Sources Sci. Technol.* **27**, 053001 (2018).
- ²⁷M. J. E. Casey, J. de Urquijo, L. N. Serkovu Loli, D. G. Cocks, G. J. Boyle, D. B. Jones, M. J. Brunger, and R. D. White, *J. Chem. Phys.* **147**, 195103 (2017).
- ²⁸G. J. Boyle, R. P. McEachran, D. G. Cocks, M. J. Brunger, S. J. Buckman, S. Dujko, and R. D. White, *J. Phys. D: Appl. Phys.* **49**, 355201 (2016).
- ²⁹M. J. Brunger, *Int. Rev. Phys. Chem.* **36**, 333 (2017).
- ³⁰S. T. Perkins, D. E. Cullen, and S. M. Saltzer, Report No. 31, Lawrence Livermore National Laboratory, 1991.
- ³¹O. Zatsarinny, K. Bartschat, G. Garcia, F. Blanco, L. R. Hargreaves, D. B. Jones, R. Murrie, J. R. Brunton, M. J. Brunger, M. Hoshino, and S. J. Buckman, *Phys. Rev. A* **83**, 042702 (2011).
- ³²K. Bartschat (private communication, 2018).
- ³³W. Adcock and M. J. Brunger, *J. Chem. Soc., Perkin Trans. 2* **2002**, 1.
- ³⁴R. Pascual, J. Mitroy, L. Frost, and E. Weigold, *J. Phys. B: At., Mol. Opt. Phys.* **21**, 4239 (1988).
- ³⁵K. Bartschat, *J. Phys. B: At., Mol. Opt. Phys.* **51**, 132001 (2018).
- ³⁶Y. Itikawa, *J. Phys. Chem. Ref. Data* **44**, 013105 (2015).
- ³⁷Y. Itikawa, *J. Phys. Chem. Ref. Data* **45**, 033106 (2016).